Asian Journal of Chemistry; Vol. 26, No. 19 (2014), 6591-6596

ASIAN JOURNAL OF CHEMISTRY

http://dx.doi.org/10.14233/ajchem.2014.16717

Supported Bimetallic Pt-M/γ-$A1_2O_3$ (M = Sn, Ce, Cr) Catalysts for Perhydrofluorene Dehydrogenation

Y. LI[1], Q. ZHAO[1], J.P. DU[2] and J.P. LI[1,*]

[1]Research Institute of Special Chemicals, Taiyuan University of Technology, Taiyuan 030024, Shanxi Province, P.R. China
[2]College of Chemistry and Chemical Engineering, Taiyuan University of Technology, Taiyuan 030024, Shanxi Province, P.R. China

*Corresponding author: Tel/Fax: +86 351 6010908; E-mail: jpli211@hotmail.com

Received: 19 November 2013; *Accepted*: 5 March 2014; *Published online*: 16 September 2014; AJC-15968

Effect of several oxide promoters (oxides of Sn, Ce and Cr) on dehydrogenation of perhydrofluorene over Pt/γ-$A1_2O_3$ catalyst was investigated. The effect of catalyst amount, temperature, carriers, loading amount were investigated. The catalysts were characterized by TEM, BET and H_2-TPR. The addition of a promoter metal, such as Sn, Ce, or Cr, to Pt/γ-$A1_2O_3$ catalyst could remarkably increased its activity and dehydrogenation conversion rate of perhydrofluorene could be raised. The optimized calcined temperature is 500 °C with the perhydrofluorene dehydrogenation conversion over 97 %. The 2.5 wt. % Pt-0.5 wt. % Sn/γ-$A1_2O_3$ catalyst 2.5 wt. % Pt-0.5 wt. % Cr/γ-$A1_2O_3$ catalyst, 2.5 wt. % Pt-2.5 wt. % Ce/γ-$A1_2O_3$ catalyst resulted in a maximum perhydrofluorene dehydrogenation capacity of 6.667 wt. %, 6.609 wt. %, 6.641 wt. % with the perhydrofluorene dehydrogenation conversion over 98 %, significantly higher than that obtained for other catalysts.

Keywords: Platinum-based catalyst, Dehydrogenation, Perhydrofluorene, Metal oxide.

INTRODUCTION

In order to meet the ever increasing energy demand without causing further damage to the environment, zero carbon emission fuel such as hydrogen is required[1,2]. Hydrogen is a fascinating energy carrier. Hydrogen being a highly flammable gas, its storage and transport involves several safety issues.

Over the past few decades, different hydrogen storage alternatives such as hydrogen compression in pressurized vessels[3], hydrogen liquefaction[4], hydrogen adsorption in metal hydrides[5-8], hydrogen physisorption materials[9,10] and hydrogen storage in liquid organic hydrides have been developed[11]. Hydrogen storage technique with liquid organic hydrides (LOH)[12] can be applied to store and transport hydrogen energy in large scale and long distance. The processes include aromatics hydrogenation and cycloalkanes dehydrogenation. liquid organic hydrides are used for transporting the hydrogen in chemical bonded form at ambient temperature and pressure[13]. The hydrogen is delivered through a catalytic dehydrogenation process. Due to simple reaction mechanism, the dehydrogenation reaction is considered as favorable process for hydrogen abstraction. As one promising approach based on Autothermal hydrogen storage and delivery system substituting the typical liquid organic hydrides, perhydrofluorene (PHF) as liquid carriers was recently proposed by air products in their patent[14]. The heat required for the release of H_2 from the hydrogenated liquid carrier is supplied by an aerobic oxidative dehydrogenation step using the dehydrogenated carrier, thus not requiring an input of heat from an external source or heat derived from burning the hydrogen. Moreover, the dehydrogenation reaction of perhydrofluorene can be operated in liquid-phase model.

Pt/γ-Al_2O_3 is a typical dehydrogenation catalysts, but Pt content of the catalyst is high. So by adding a second metal in the preparation of bimetallic catalyst solve this problem which reduce the amount of noble metal and obtain low cost recycling catalyst with high conversion rate and high stability. The second metal may influence the first metal through electronic interactions or be involved in the reaction by bonding directly to reactants or intermediates. Often, the interactions between the two metals are complex and largely unknown and consequently there are excellent opportunities for preparing bimetallic complex and largely unknown and consequently there are excellent opportunities for preparing bimetallic catalysts with new properties. The second metal may substantially suppress the amount of hydrogen chemisorbed on the surfaces of bimetallic particles, much as it affects the catalytic properties for some reactions. Some bimetallic catalysts have better thermal stabilities and resistance to deactivation than catalysts incorporating only the single metals.

In this paper, the effects of moderate amount of the second metal addition into the reaction of catalytic dehydrogenation to modified Pt/γ-Al_2O_3 catalysts were investigated. Their

catalytic properties over liquid organic perhydrofluorene (PHF) have been investigated. The additive effects of Sn, Ce and Cr were characterized by BET, TPR and TEM.

EXPERIMENTAL

The chemical reagents used in the experiments were as follows: stannic chloride ($SnCl_4·5H_2O$, 99.5 %, Aldrich), cerium(III) nitrate hexahydrate [$Ce(NO_3)_3·6H_2O$, 99.95 %, Aldrich], chromium(III) nitrate nonahydrate [$Cr(NO_3)_3·9H_2O$, 99.9 %, Aldrich], cyclohexane (≥ 99.9 %, Aldrich), perhydrofluorene ($C_{13}H_{22}$, 97 %, Aldrich) and chloroplatinic acid hydrate ($H_2PtCl_6·6H_2O$, 99.9 %, Aldrich). They were obtained from the indicated commercial sources and used without further purification. Distilled water was prepared in our laboratory.

Catalysts preparation: Catalysts were prepared *via* incipient wetness impregnation. The γ-alumina was used as the support. Pt/γ-Al_2O_3 catalyst was prepared by impregnating γ-Al_2O_3 with equivalent aqueous solution of the Pt precursor ($H_2PtCl_6·6H_2O$) . After impregnation, the catalyst was dried at 120 °C for 12 h and then calcined at 500 °C in air for 4 h. For Pt-Sn/γ-Al_2O_3, Pt-Ce/γ-Al_2O_3 and Pt-Cr/γ-Al_2O_3 catalysts, Sn, Ce or Cr was first deposited by impregnating with ethanolic solution of $SnCl_4·5H_2O$, $Ce(NO_3)_3·6H_2O$ and $Cr(NO_3)_3·9H_2O$ dissolved in distilled water. Followed by drying and calcination and finally, the Pt component was added from aqueous solution of Pt in a similar way. The hydrogen reduction was carried out at different temperature and then the bimetallic catalysts were successfully obtained. Samples were degassed at room temperature for 0.5 h in flowing hydrogen in pipe furnace, reducted with the temperature increasing at a rate of 10 °C/min from room temperature to the specified temperature for 2.5 h and finally protected by flowing argon.

Catalytic dehydrogenation of perhydrofluorene: Under an argon atmosphere, 4 g of perhydrofluorene and different amount of Pt-M/γ-Al_2O_3 were placed in a stirred reactor (egg plant-shaped-flask, 25 mL) and the reactor was sealed. The reactor was connected to a manifold containing a vacuum source, hydrogen source and hydrogen measurement system. After evacuation of residual air from the manifold lines, hydrogen was purged through the reactor to displace the argon from the reactor headspace. Catalytic dehydrogenation of perhydrofluorene in reactor was performed under oil bath heated at different temperature. Evolved hydrogen was collected into a gas burette and quantified volumetrically. Reaction rates were obtained from the evolved amount of gaseous hydrogen continuously, while the final conversion of the substrate was determined by GC analysis of the residual condensates at the final stage of reaction.

Characterization: N_2 adsorption was measured with an ASAP 2020 gas-adsorption apparatus at liquid-nitrogen temperature. Samples were dehydrated under vacuum at 200 °C overnight prior to the experiments. The transmission electron microscopy (TEM) was carried out by using JEOL JEM-2100F instrument operated at 200 kV. The sample was suspended in ethanol and sonicated for 1 h. Subsequently a drop of the suspended sample was placed on a cooper grid for analysis. Temperature programmed reduction(TPR) was measured with AutoChen II 2920. For the experiments, 10 % H_2 in Ar was used as the preparation gas and Ar was used as the carrier/reference gas. Samples were degassed at 100 °C for 1 h in flowing argon to remove water vapor. The samples were then temperature programmed to 500 °C at a ramp rate of 10 °C/min and held at that temperature for 0.5 h to remove strongly bound species and activate the sample. After cooling to room temperature in a stream of flowing argon and switching to hydrogen(10 % H_2 in argon, 30 mL/min), the temperature was increased (5 °C/min) to 700 °C. And the amount of H_2 consumed was determined with a thermal conductivity detector (TCD).

RESULTS AND DISCUSSION

Dehydrogenation properties of perhydrofluorene over Pt-M/γ-Al_2O_3: The dehydrogenation properties of the perhydrofluorene (PHF) was carried out on each different Pt-M/γ-Al_2O_3 (M = Sn, Ce and Cr) catalysts. Figs. 1-3 and Tables 1-3 show the dehydrogenation properties of the perhydrofluorene at 235 °C over different M content catalysts with Pt-M/γ-Al_2O_3 (M = Sn, Ce and Cr). The data indicate that the dehydrogenation capacity of perhydrofluorene decreases gradually along with the increase in the content of Sn, Cr and the decrease in the content of Ce due to the lower dispersion and agglomeration of platinum on the support surface. The 2.5 wt. % Pt-0.5 wt. % Sn/γ-Al_2O_3 catalyst, 2.5 wt. % Pt-0.5 wt. % Cr/γ-Al_2O_3 catalyst, 2.5 wt. % Pt-2.5 wt. % Ce/γ-Al_2O_3 catalyst resulted in a maximum perhydrofluorene dehydrogenation capacity of 6.667 wt. %, 6.609 wt. %, 6.641 wt. % with the perhydrofluorene dehydrogenation conversion over 98 %, significantly higher than that obtained for other catalysts.

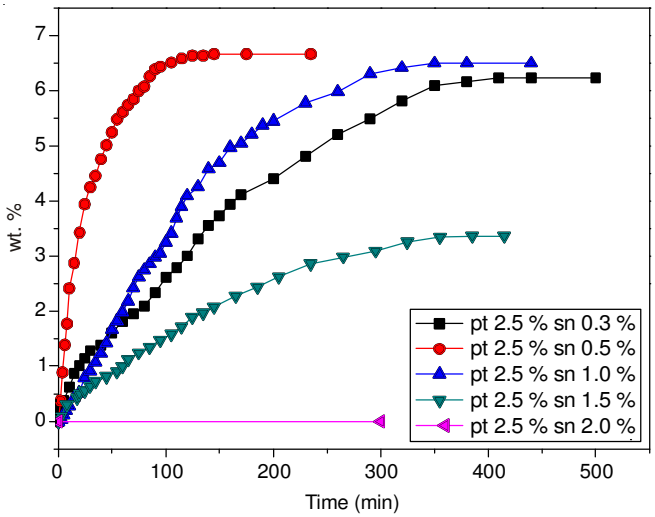

Fig. 1. Effect of Sn content on perhydrofluorene (PHF) dehydrogenation over Pt-Sn/γ-Al_2O_3

Effect of calcined temperature on catalytic activity of Pt-M/γ-Al_2O_3: Above the experiment, we have to obtain the best content of the second metal in Pt-M/γ-Al_2O_3 (M = 0.5 wt. % Sn, 2.5 wt. % Ce, 0.5 wt. % Cr). Then we hope find the optimized calcined temperature of Pt-M/γ-Al_2O_3 (M = 0.5 wt. % Sn, 2.5 wt. % Ce, 0.5 wt. % Cr). The effect of calcined temperature of catalyst preparation on the dehydrogenation was examined over

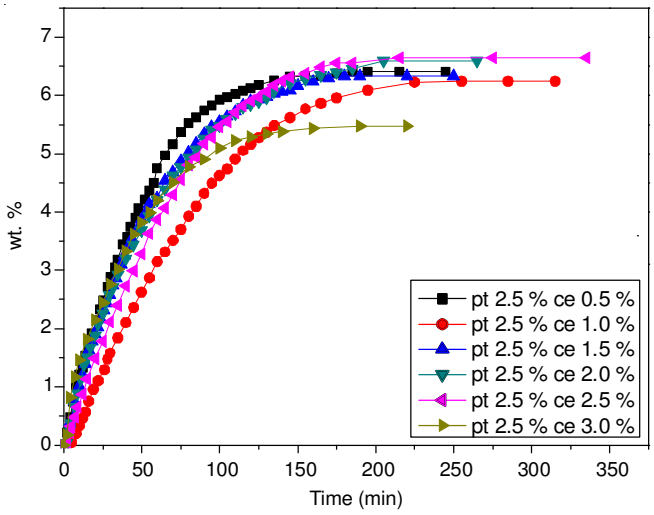

Fig. 2. Effect of Ce content on perhydrofluorene (PHF) dehydrogenation over Pt-Ce/γ-Al_2O_3

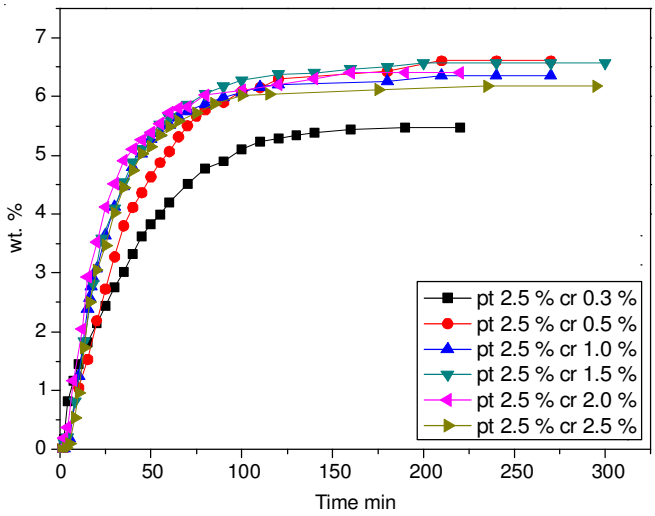

Fig. 3. Effect of Cr content on perhydrofluorene (PHF) dehydrogenation over Pt-Cr/γ-Al_2O_3

TABLE-1
DEHYDROGENATION PRODUCTS ANALYSIS OF PERHYDROFLUORENE OVER DIFFERENT Pt-Sn/γ-$A1_2O_3$ CATALYSTS

Catalysts	Catalyst nominal composition (wt. %)		Dehydrogenation capacity (wt. %)	Conversion (%)
	Pt	Sn		
1	2.5	0	5.331	79.07
2	2.5	0.3	6.230	92.41
3	2.5	0.5	6.667	98.88
4	2.5	1.0	6.496	96.35
5	2.5	1.5	3.367	49.94
6	2.5	2.0	0	0

400, 500, 600, 700 and 800 °C, respectively. As shown in Figs. 4-6, as the calcined temperature increased, dehydrogenation conversion of perhydrofluorene increased before they are reduced, the optimized calcined temperature is 500 °C with the perhydrofluorene dehydrogenation conversion over 97 %. In addition, Pt-Sn/γ-Al_2O_3 and Pt-Cr/γ-Al_2O_3 have been inactivity over 700 °C and Pt-Ce/γ-Al_2O_3 have been inactivity over 800 °C. This result also demonstrates that the calcined

TABLE-2
DEHYDROGENATION PRODUCTS ANALYSIS OF PERHYDROFLUORENE OVER DIFFERENT Pt-Ce/γ-$A1_2O_3$ CATALYSTS

Catalysts	Catalyst nominal composition (wt. %)		Dehydrogenation capacity (wt. %)	Conversion (%)
	Pt	Ce		
1	2.5	0	5.331	79.07
2	2.5	0.5	6.407	95.03
3	2.5	1.0	6.242	92.58
4	2.5	1.5	6.325	93.82
5	2.5	2.0	6.590	97.75
6	2.5	2.5	6.641	98.50
7	2.5	3.0	5.473	81.18

TABLE-3
DEHYDROGENATION PRODUCTS ANALYSIS OF PERHYDROFLUORENE OVER DIFFERENT Pt-Cr/γ-$A1_2O_3$ CATALYSTS

Catalysts	Catalyst nominal composition (wt. %)		Dehydrogenation capacity (wt. %)	Conversion (%)
	Pt	Cr		
1	2.5	0	5.331	79.07
2	2.5	0.3	6.045	89.66
3	2.5	0.5	6.609	98.03
4	2.5	1.0	6.356	94.27
5	2.5	1.5	6.565	97.37
6	2.5	2.0	6.401	94.94
7	2.5	2.5	6.172	91.55

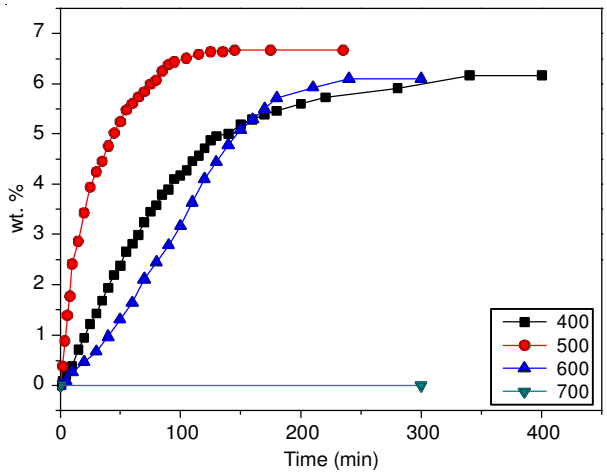

Fig. 4. Effect of calcined temperature on catalyst preparation of Pt-Sn/γ-Al_2O_3

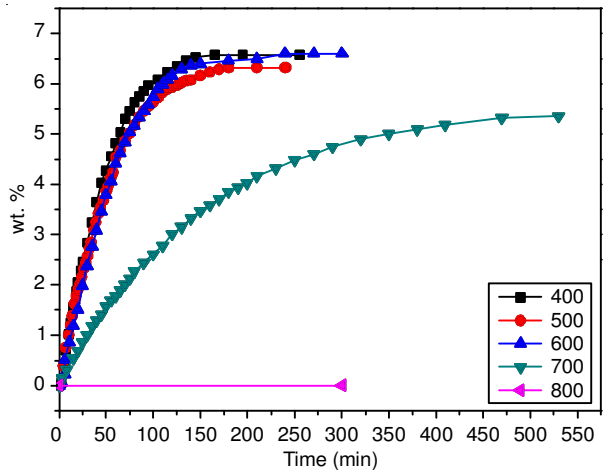

Fig. 5. Effect of calcined temperature on catalyst preparation of Pt-Ce/γ-Al_2O_3

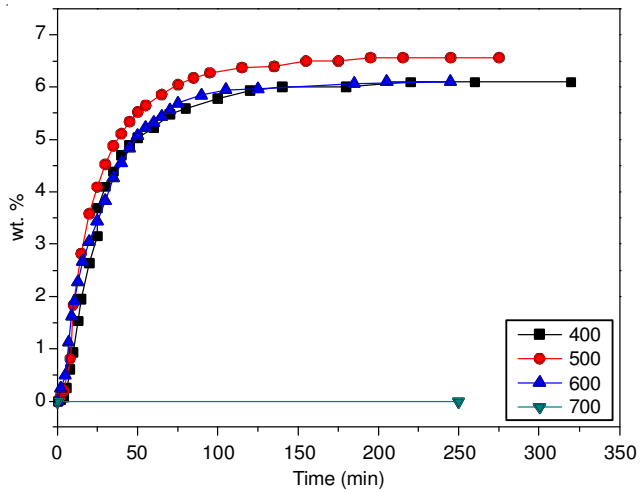

Fig. 6. Effect of calcined temperature on catalyst preparation of Pt-Cr/γ-Al_2O_3

temperature has impact on the final dehydrogenation capacity. The final dehydrogenation capacity is shown in Tables 4-6.

TABLE-4
EFFECT OF CALCINED TEMPERATURE ON PERHYDROFLUORENE DEHYDROGENATION OVER Pt-Sn/γ-$A1_2O_3$

Catalysts	Calcined temperature (°C)	Dehydrogenation capacity (wt. %)	Conversion (%)
1	400	6.172	91.55
2	500	6.667	98.89
3	600	6.102	90.51
4	700	0	0

TABLE-5
EFFECT OF CALCINED TEMPERATURE ON PERHYDROFLUORENE DEHYDROGENATION OVER Pt-Ce/γ-$A1_2O_3$

Catalysts	Calcined temperature (°C)	Dehydrogenation capacity (wt. %)	Conversion (%)
1	400	6.578	97.57
2	500	6.603	97.94
3	600	6.325	93.81
4	700	5.357	79.46
5	800	0	0

TABLE-6
EFFECT OF CALCINED TEMPERATURE ON PERHYDROFLUORENE DEHYDROGENATION OVER Pt-Cr/γ-$A1_2O_3$

Catalysts	Calcined temperature (°C)	Dehydrogenation conversion (wt. %)	Conversion (%)
1	400	6.089	90.31
2	500	6.565	97.37
3	600	6.096	90.42
4	700	0	0

Comparision of different the second metal on optimum loading: As shown in Fig. 7, the reaction rate is obvious different in the first 50 min, the trend is declined slightly in the 100 min, three lines are almost overlap and no longer change over 200 min. Final dehydrogenation capacity have a small gap with the perhydrofluorene dehydrogenation conversion over 98 %. The addition of CeO_2, SnO_2 and CrO_2 to Pt/γ-Al_2O_3 catalyst could greatly increase its activity and conversion of perhydrofluorene (PHF) could be raised and also accelerated the rate of dehydrogenation. These results confirm in Table-7 that, compared with other two kinds of added metal, the reaction rate of Sn is quick, the balance of time is relatively short. And Ce and Cr, the reaction rate and equilibrium time should be longer.

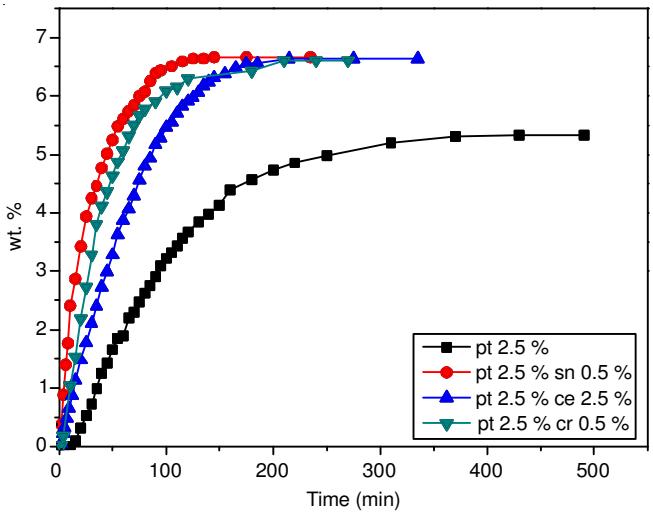

Fig. 7. Effect of different optimum loading on catalyst preparation of Pt-M/γ-Al_2O_3

Temperature-programmed reduction: The states of the metals and the interactions of the metal (oxides) components among themselves and with the supports are investigated by H_2-TPR. Temperature-programmed reduction experiments provide insight into the proximity of metallic phases through the observation of shifts in reduction peaks as compared to monometallic catalysts. Fig. 8 shows the TPR profiles for the Pt/γ-Al_2O_3 and corresponding bimetallic Pt-Sn/γ-Al_2O_3, Pt-Ce/γ-Al_2O_3 and Pt-Cr/γ-Al_2O_3 catalysts. The Pt/γ-Al_2O_3 catalyst shows an increase of hydrogen consumption in the Pt reduction region, particularly near 220 °C. All the TPR profiles of the catalysts (Fig. 8b,c,d) exhibit two temperature reduction peaks. The first H_2 consumption peak would correspond to the reduction of the Pt oxide, which is distributed among smaller crystals and with mild interaction with supports. When adding a second metal, reduction temperature of Pt is down to

TABLE-7
EFFECT OF DIFFERENT OPTIMUM LOADING ON CATALYST PREPARATION OF Pt-M/γ-$A1_2O_3$ (M = Sn, Ce AND Cr)

Catalysts	Catalyst nominal composition (wt. %)		Dehydrogenation conversion under different reaction time (wt. %)		
	Pt	Second metal	50 min	100 min	≥ 200 min
Pt/γ-$A1_2O_3$	2.5	0	1.657	3.216	5.331
Pt-Sn/γ-$A1_2O_3$	2.5	0.5	5.250	6.512	6.667
Pt-Ce/γ-$A1_2O_3$	2.5	2.5	3.277	5.463	6.641
Pt-Cr/γ-$A1_2O_3$	2.5	0.5	4.628	6.086	6.609

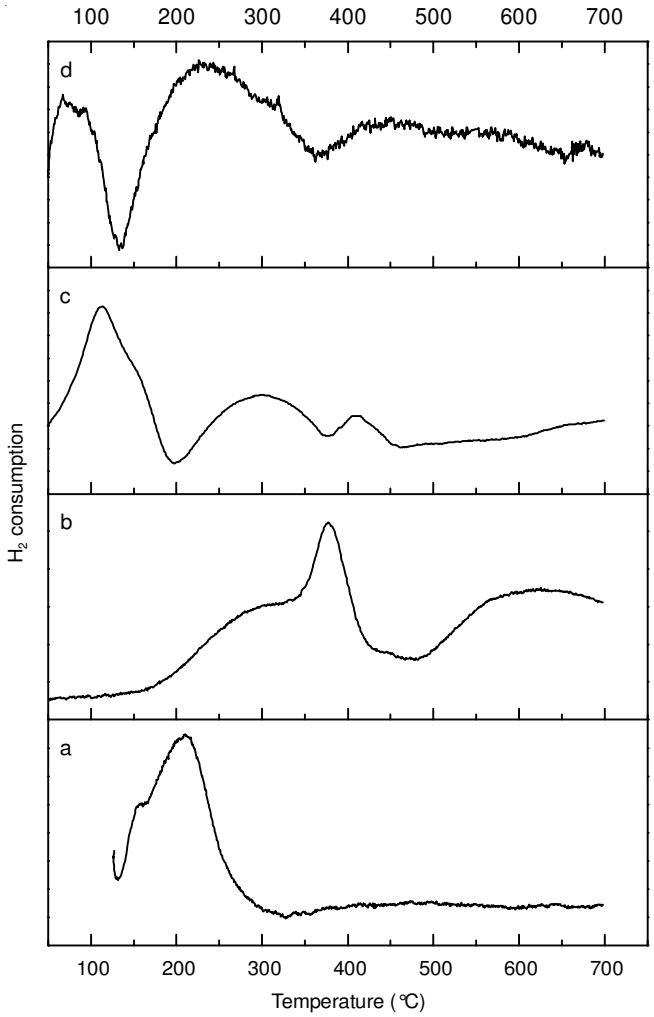

Fig. 8. H_2-temperature programmed reduction (TPR) spectra of catalysts, a. Pt/γ-Al_2O_3; b. Pt-Sn/γ-Al_2O_3; c. Pt-Ce/γ-Al_2O_3; d. Pt-Cr/γ-Al_2O_3 (Sn, Ce and Cr as their oxides, respectively)

about 120 °C. Such a shift in reduction temperature is typical of close Pt-M intimacy, possibly in the form of Pt_xM alloys. Therefore this fraction of M oxides in direct interaction with Pt is reduced at the Pt reduction temperature. The second reduction peak at the maximum temperature of catalysts corresponds to the reduction of Sn, Ce and Cr.

Transmission electron microscopy: The typical Pt-M/γ-Al_2O_3 (M = Sn, Ce and Cr) samples were characterized by TEM. Fig. 9 images of samples with 2.5 wt. % Pt-0.5 wt. % Sn/γ-Al_2O_3, 2.5 wt. % Pt-2.5 wt. % Ce/γ-Al_2O_3 and 2.5 wt. % Pt-0.5 wt. % Cr/γ-Al_2O_3. For doped sample, the dark spots of Pt particles could be observed. The uniform dispersion and small particles with the size mainly between 10 and 20 nm were found for the catalyst samples. These results confirm that the Pt nanoparticles have been successfully doped into the cavities of the γ-Al_2O_3 support. It is worth noting that matching the cavity size is important for preventing the particle from further growing and aggregation. Otherwise it is difficult to obtain the small platinum particles outside the cavities of γ-Al_2O_3 due to the weak metal-support interaction[15]. In addition, the dark spots of Pt-Sn/γ-Al_2O_3 sample are more uniformly well-distributed than the Pt-Ce/γ-Al_2O_3 and Pt-Cr/γ-Al_2O_3 sample, suggesting the more active sites obtained for Pt-Sn/γ-Al_2O_3. Compared with other two kinds of catalysts, the size of the Pt particles also observes obviously.

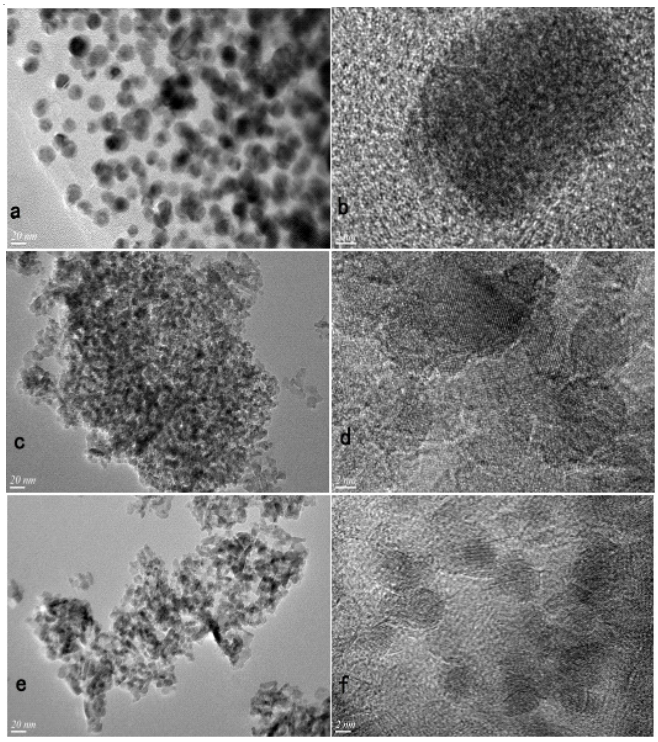

Fig. 9. Transmission electron microscopy (TEM) images of Pt-M/γ-Al_2O_3 (M = Sn, Ce and Cr), (a, b: Pt-Sn/γ-Al_2O_3 (2.5 wt.% Pt, 0.5 wt. % Sn); c, d: Pt-Ce/γ-Al_2O_3 (2.5 wt. % Pt, 2.5 wt. % Ce); e, f: Pt-Cr/γ-Al_2O_3 (2.5 wt. % Pt, 0.5 wt. % Cr)

N_2 adsorption analysis: The pore properties of catalyst were analyzed based on the nitrogen adsorption. The BET surface area, pore volume and pore diameter of the samples prepared are given in Table-8. The structure parameters of Pt-Sn/γ-Al_2O_3 were then derived with the BET surface area of 154.6 m^2 g^{-1}, the total pore volume of 0.82 cm^3 g^{-1} and the average pore diameter of 21.09 nm. The structure parameters of Pt-Sn/γ-Al_2O_3 with the BET surface area of 155.2 m^2 g^{-1}, total pore volume of 0.62 cm^3 g^{-1} and pore diameter of 21.12 nm. The structure parameters of Pt-Cr/γ-Al_2O_3 were then

TABLE-8
STRUCTURE PARAMETERS OF CATALYSTS

Catalysts	Catalyst nominal composition (wt. %)		BET measurement		
	Pt	Second metal	BET Surface Area (m^2 g^{-1})	Pore volume (cm^3 g^{-1})	Pore Diameter (nm)
γ-$A1_2O_3$	0	0	152.7	0.69	18.13
Pt-Sn/γ-$A1_2O_3$	2.5	0.5	154.6	0.82	21.09
Pt-Ce/γ-$A1_2O_3$	2.5	2.5	155.2	0.82	21.12
Pt-Cr/γ-$A1_2O_3$	2.5	0.5	150.7	0.68	18.09

derived with the BET surface area of 150.73 $m^2 g^{-1}$, the total pore volume of 0.68 $cm^3 g^{-1}$ and the average pore diameter of 18.09 nm. The obvious change in surface area indicates that the cavities of the host framework are occupied by highly dispersed Pt nanoparticles and blocked by Pt nanoparticles locating at the surface.

Conclusion

In summary, a Pt-M/γ-Al_2O_3 (M = Sn, Ce and Cr) was employed as a support for preparing nanoparticle platinum catalysts by a simple incipient impregnation method, which was used as a catalyst in the liquid phase perhydrofluorene dehydrogenation and exhibited considerable activity. Effect of several oxide promoters (oxides of Sn, Ce and Cr) on dehydrogenation of perhydrofluorene over Pt/γ-Al_2O_3 catalyst was investigated. Most of promoters could improve catalytic performance of Pt/γ-Al_2O_3 in perhydrofluorene dehydrogenation. The 2.5 wt. % Pt-0.5 wt. % Sn/γ-Al_2O_3 catalyst, 2.5 wt. % Pt-0.5 wt. % Cr/γ-Al_2O_3 catalyst, 2.5 wt. % Pt-2.5 wt. % Ce/γ-Al_2O_3 catalyst resulted in a maximum perhydrofluorene dehydrogenation capacity of 6.667 wt. %, 6.609 wt. %, 6.641 wt. % with the perhydrofluorene dehydrogenation conversion over 98 %, significantly higher than that obtained for other catalysts. The optimized calcined temperature is 500 °C with the perhydrofluorene dehydrogenation conversion over 97 %. In transmission electron microscopy the particles are well-distributed and small over Pt-Sn/γ-Al_2O_3 catalyst and catalytic activity is also optimized. It is hoped that particles of Ce or Cr will be well-distributed and small to improve their activity.

ACKNOWLEDGEMENTS

The authors gratefully acknowledged the financial support from the National Natural Science Foundation of China (No. 51002103, 21476153, 21136007), the Natural Science Foundation of Shanxi Province (2014011017-1) and the Program for the Outstanding Innovative Teams of Higher Learning Institutions of Shanxi.

REFERENCES

1. R.M. Navarro Yerga, M.C. Álvarez Galván, F. Del Valle, J.A. Villoria De La Mano and J.L.G. Fierro, *ChemSusChem*, **2**, 471 (2009).
2. W. Wang, Q. Zhao, J.X. Dong and J.P. Li, *Int. J. Hydrogen Energy*, **36**, 7374 (2011).
3. B.P. Xu, J.X. Wen, S. Dembele, V.H.Y. Tam and S.J. Hawksworth, *J. Loss Prevent Proc.*, **22**, 279 (2009).
4. H. Huang, K.Y. Wang, S.J. Wang, M.T. Klein and W.H. Calkins, *Energy Fuels*, **10**, 641 (1996).
5. K. Srinivasu and S.K. Ghosh, *Int. J. Hydrogen Energy*, **36**, 15681 (2011).
6. D.J. Wolstenholme, J.T. Titah, F.N. Che, K.T. Traboulsee, J. Flogeras and G.S. McGrady, *J. Am. Chem. Soc.*, **133**, 16598 (2011).
7. I.P. Jain, P. Jain and A. Jain, *J. Alloys Comp.*, **503**, 303 (2010).
8. S. Kalinichenka, L. Röntzsch and B. Kieback, *Int. J. Hydrogen Energy*, **34**, 7749 (2009).
9. J.X. Dong, X.Y. Wang, H. Xu, Q. Zhao and J.P. Li, *Int. J. Hydrogen Energy*, **32**, 4998 (2007).
10. J.P. Li, S.J. Cheng, Q. Zhao, P.P. Long and J.X. Dong, *Int. J. Hydrogen Energy*, **34**, 1377 (2009).
11. S. Orimo, Y. Nakamori, J.R. Eliseo, A. Züttel and C.M. Jensen, *Chem. Rev.*, **107**, 4111 (2007).
12. F. Alhumaidan, D. Cresswell and A. Garforth, *Energy Fuels*, **25**, 4217 (2011).
13. A.U. Pradhan, A. Shukla, J.V. Pande, S. Karmarkar and R.B. Biniwale, *Int. J. Hydrogen Energy*, **36**, 680 (2011).
14. O.S. Alexeev and B.C. Gates, *Ind. Eng. Chem. Res.*, **42**, 1571 (2003).
15. S. Hermes, M. Schröter, R. Schmid, L. Khodeir, M. Muhler, A. Tissler, R.W. Fischer and R.A. Fischer, *Angew. Chem. Int. Ed.*, **44**, 6237 (2005).